BRITISH ECOLOGICAL SOCIETY Functional Ecology

The negative effects of an allelopathic invader on native plant photosynthesis intensify as the growth season progresses

Journal:	*Functional Ecology*
Manuscript ID	FE-2025-00191
Wiley - Manuscript type:	Research Article
Key-words:	Alliaria petiolata, AM fungi, plant invasion, stomatal conductance, J_{max}, V_{max}

"The negative effects of an allelopathic invader on native plant photosynthesis intensify as the growth season progresses"

Abstract

1. Many invasive plants produce allelopathic compounds that disrupt plant-fungal symbioses in native species, influencing nutrient and water provisioning to support photosynthesis. Previous studies have linked these disruptions to reductions in photosynthesis and stomatal conductance, but no study has quantified whether these effects are also tied to reductions in photosynthetic capacity, limiting inferences about the mechanisms driving these responses. Furthermore, no study has quantified how these responses vary temporally across the growing season.
2. To investigate the temporal dynamics that drive native plant responses to allelopathic invasion, we measured gas exchange in two understory native species (*Trillium* spp. and *Maianthemum racemosum*) at two points during the growing season – once early in the growing season while the tree canopy was open and again later in the growing season when the tree canopy was closed. Measurements were collected in a long-term field experiment where *Alliaria petiolata*, an allelopathic invader that disrupts AM fungal communities, has been hand-weeded or left at ambient levels since 2006.
3. Both native species exhibited significantly reduced net photosynthesis rates under ambient *A. petiolata* levels compared to the weeded treatment. In *Trillium* spp., this response was due to a reduction in apparent photosynthetic capacity. In *M. racemosum*, this response was due to a reduction in stomatal conductance that increased in stomatal limitation. In both species, photosynthetic responses to the allelopathic invader were strongest later in the growing season.
4. Our findings indicate that *A. petiolata* reduces native plant net photosynthesis either by increasing nutrient stress, as indicated by the reduction in apparent photosynthetic capacity in *Trillium* spp., or by increasing water stress, as indicated by the reduction in stomatal conductance in *M. racemosum*. Regardless of mechanism, both species demonstrated stronger negative photosynthetic responses to *A. petiolata* later in the growing season, highlighting the importance of quantifying the temporal dynamics that regulate plant physiological responses to allelopathic invaders. While not quantified in

this study, amplified late-season responses to *A. petiolata* may have been associated with increased reliance on disrupted AM fungal partners for soil resources, as soil nutrient availability and soil moisture each declined as the growing season progressed.

Keywords
Alliaria petiolata, AM fungi, photosynthesis, plant invasion, stomatal conductance, V_{cmax}, J_{max}

Introduction

Invasive plants often express unique traits that increase their likelihood of establishment in novel ecosystems. Allelopathy, defined as a secondary compound produced by a plant that negatively impacts neighboring plant species and/or soil microbial communities (Inderjit et al., 2011), has emerged as a mechanism to explain the success of some invasive plant species (Callaway et al., 2008; Callaway & Ridenour, 2004). Allelopathy negatively affects native plant performance and soil microbial community composition (Bialic-Murphy et al., 2020, 2021; Brouwer et al., 2015; Hale et al., 2011, 2016; Hale & Kalisz, 2012; Qu et al., 2021; Roche et al., 2021; Zhang et al., 2021) and is estimated to occur in approximately 52% of invasive plant species (Kalisz et al., 2021). Despite the prevalence of allelopathy among invasive species, our understanding of the mechanisms that drive physiological responses of coexisting native species to allelopathic invasion and the temporal dynamics that underpin these responses remains limited. This knowledge gap hinders our understanding of how the disruptive impacts of allelopathic invasion on soil microbial communities scale to influence plant community dynamics.

Photosynthesis links ecosystem carbon, nutrient, and water cycles in terrestrial ecosystems (Hungate et al., 2003). Through photosynthesis, plants convert carbon dioxide into simple sugars using enzymes such as Ribulose-1,5-bisphosphate carboxylase/oxygenase (Rubisco) that require large amounts of nutrients and energy to build and maintain (Evans & Clarke, 2019; Evans & Seemann, 1989). Aboveground conditions such as light availability, atmospheric CO_2 concentration, vapor pressure deficit, and temperature regulate photosynthetic enzyme kinetics and substrate availability, rendering these factors key determinants of plant demand to acquire and allocate nutrients toward the construction and maintenance of photosynthetic enzymes and demand to maintain transpiration streams needed to support photosynthesis (Bernacchi et al., 2001; Dong et al., 2017, 2020, 2022; Paillassa et al., 2020; N.

G. Smith et al., 2019; Westerband et al., 2023). Whether plants can satisfy this demand in a given environment depends on nutrient and water availability, and the uptake and allocation of these resources to photosynthetic tissues. For example, increased light availability often increases the demand for soil nutrients and water to enhance photosynthetic capacity and stomatal conductance to optimize light use (N. G. Smith et al., 2019; Walters, 2005). In resource-rich environments, plants can meet this increased demand by increasing nutrient and water uptake and allocating these resources to photosynthetic processes. However, plants cannot increase nutrient and water uptake to a similar extent in resource-limited environments, as resource availability is insufficient to acquire and satisfy the demand for photosynthetic enzymes. This scenario could cause individuals growing in resource-limited environments to display reduced physiological responses to increased light availability compared to individuals growing in resource-rich environments (Waring et al., 2023) and could increase plant reliance on symbioses with soil microbial communities (e.g., mycorrhizal fungi) for soil resources (Treseder, 2004; van Diepen et al., 2007).

Allelopathic compounds with antimicrobial properties can inhibit the growth and reproduction of soil microbial communities, such as mycorrhizal fungi, which are essential for providing nutrients and water to their host plants (Hale & Kalisz, 2012). Arbuscular mycorrhizal (AM) fungi form obligate symbioses with plants, exchanging mineral nutrients and water for photosynthate (S. E. Smith & Read, 2008). Antimicrobial compounds produced by allelopathic invaders can disrupt these symbioses by inhibiting AM fungal spore germination, fungal root colonization, and arbuscule formation, which can decrease AM fungal biomass, alter AM fungal species richness, and modify AM fungal community composition (Burke, 2008; Callaway et al., 2008; Burke et al., 2011; Cantor et al., 2011; Anthony et al., 2019; Bialic-Murphy et al., 2021). These disruptions can lead to decreased nutrient and water uptake in plants that rely on AM fungi, even when allelopathic invaders do not directly modify ecosystem nutrient or water availability (Bialic-Murphy et al., 2021). This is because disruptions in AM fungal mutualisms may increase the plant carbon cost for acquiring nutrients and water, causing plants to receive less resources provisioned by AM fungal partners for a given belowground carbon investment (Hale et al., 2016; Kummel & Salant, 2006). This pattern may scale to alter resource allocation to photosynthetic enzymes, as emerging evidence suggests that increased costs of nutrient acquisition are associated with altered nutrient allocation to photosynthetic enzymes (Perkowski

et al., 2021; Waring et al., 2023). Thus, disruptions in AM fungal mutualisms could cause native plants to be unable to satisfy the demand to build and maintain photosynthetic enzymes and/or maintain optimal stomatal conductance, which may explain why native species exhibit reduced net photosynthesis rates in response to allelopathic invaders (Hale et al., 2011, 2016).

Alliaria petiolata (M. Bieb) Cavara & Grande (Family: Brassicaceae) is a model species for investigating the impacts of allelopathic plant invasion on native plant communities. This biennial herb from Eurasia invades temperate forest understories in North America, releasing glucosinolates into soil environments through root exudation and leaf litter (Rodgers et al., 2008). Glucosinolates produced by *A. petiolata* hydrolyze into antimicrobial compounds such as allyl isothiocyanate, which inhibit AM spore germination, spore viability, root colonization, and arbuscule formation (Anthony et al., 2019; Callaway et al., 2008; Cantor et al., 2011). Previous work has linked *A. petiolata* invasion with decreased AM fungal biomass, increased AM species richness, and altered fungal community composition (Bialic-Murphy et al., 2021; Burke, 2008; Burke et al., 2011; Cantor et al., 2011). Disrupted AM fungal communities due to *A. petiolata* invasion have also been associated with negative impacts on native plant nutrient and water economics, population dynamics, and community composition (Bialic-Murphy et al., 2020, 2021; Hale et al., 2016; Roche et al., 2021, 2023), with stronger negative impacts in native species that associate with AM fungi compared to those that do not (Callaway et al., 2008; Roche et al., 2021, 2023). These patterns occur despite evidence that *A. petiolata* invasions do not affect soil nutrient or water availability, suggesting that the breakdown of the AM fungal mutualism is the mechanism that drives native plant community responses to *A. petiolata* invasion (Bialic-Murphy et al., 2021; Burke et al., 2019).

Previous work also indicates that *A. petiolata* reduces the net photosynthesis rates of a common coexisting native species, *M. racemosum*, through a reduction in stomatal conductance (Brouwer et al., 2015; Hale et al., 2011, 2016). However, the mechanisms that regulate these responses are not fully understood, in part because such studies have not quantified photosynthetic capacity responses to *A. petiolata*. Photosynthetic responses to *A. petiolata* invasion could be driven by changes in photosynthetic capacity, indicating nutrient limitation, or by changes in stomatal conductance, indicating water limitation. Understanding whether changes in photosynthetic capacity or stomatal conductance drive native plant photosynthetic responses to *A. petiolata* invasion would provide valuable insight into the mechanism underlying these

responses. Furthermore, existing field research has primarily quantified photosynthetic responses to *A. petiolata* invasion at a single time point in the growth season, providing limited insight into the impacts of allelopathic plant invasion across the growth season as understory light availability and soil resource availability decrease. Studies that investigate the mechanisms that explain the photosynthetic responses to allelopathic invaders at different time points in the growing season would be valuable for assessing how leaf-level physiological responses to allelopathic plant invasion compare to its finer-scale impacts on AM fungal community composition and broader-scale effects on native plant productivity and survivorship.

Here, we assessed the temporal dynamics that drive the effects of allelopathic invasion on leaf-level photosynthetic processes of two coexisting native plant species growing with and without the presence of *Alliaria petiolata*. To do this, we collected gas exchange measurements from two understory native species growing in a long-term *A. petiolata* field manipulation experiment. Gas exchange measurements were collected at two time points across the growing season: once early in the growth season while the tree canopy was open and again later in the growth season when the tree canopy was closed. At each measurement timepoint, we quantified net photosynthesis and stomatal conductance rates, stomatal limitation of net photosynthesis, apparent photosynthetic capacity, and relative chlorophyll content in plots where *A. petiolata* was either left at natural densities or manually removed. Throughout the measurement periods, we also quantified soil nutrient availability and continuously monitored soil moisture. We used this experiment and sampling approach to test the following hypotheses:

1) Both native species will experience a reduction in net photosynthesis in the *A. petiolata*-ambient treatment compared to the *A. petiolata*-weeded treatment. These patterns will be associated with reduced apparent photosynthetic capacity, relative chlorophyll content, and stomatal conductance, in the *A. petiolata*-ambient treatment. We expected that a reduction in apparent photosynthetic capacity and/or relative chlorophyll content in response to *A. petiolata* presence would be indicative of nutrient stress, while a reduction in stomatal conductance and increase in stomatal limitation in response to *A. petiolata* presence would be indicative of water stress.
2) The negative effects of *A. petiolata* on the photosynthetic traits of native species will depend on the measurement time point.

a) The negative effects of *A. petiolata* treatment on leaf photosynthetic traits will be strongest early in the growing season when photosynthetic demand for soil resources is highest (i.e., due to increased understory light availability). Disrupted AM fungal symbioses will create resource stress, making it more difficult for AM-associating plants to acquire nutrients and water needed to satisfy photosynthetic demand for soil resources.
b) Alternatively, the negative effects of *A. petiolata* treatment on photosynthetic traits will be strongest later in the growing season. This response may be driven by increased reliance on disrupted AM fungal partners for soil nutrients and water as resources deplete. However, as tree canopy closure reduces light availability, photosynthetic demand for soil resources may also decline, potentially mitigating the effects of AM fungal disruption on late-season physiology.

Materials and Methods

Study site and experimental design

This study was conducted at Trillium Trail Nature Reserve in Fox Chapel, PA (40.520 °N, -79.901 °W). The mean annual precipitation of the study area is 1006 mm yr^{-1} and the mean annual temperature is 11°C (2006-2020 U.S. Climate Normals; Palecki et al., 2021). Wire fences (2.5 m tall) were set up in 2002 at five 14 x 14 m experimental plots to exclude deer and other macroherbivores while allowing free movement of small mammals and birds. *Alliaria petiolata* was manually weeded at the beginning of each growth season from one half of each experimental plot since 2006, with *A. petiolata* remaining at natural densities in the other half of each plot. Manual weeding has been an effective strategy for *A. petiolata* removal, with relative abundance of *A. petiolata* averaging 0.08% in years that followed the initial weeding treatment in 2006 (Roche et al., 2021). This long-term split-plot experiment is located on 25-75% grade slopes. Soils were classified as Gilpin-Upshur-Atkins soils with dominant shale, sandstone, and red clay shale bedrock components. *Alliaria petiolata* treatments were set up parallel to the slope to prevent allelochemical leaching into the weeded side of the plot. Previous work conducted in this experiment has shown that *A. petiolata*-ambient plots exhibit decreased AM fungal biomass, decreased AM root colonization rates, and increased AM fungal richness compared to *A. petiolata*-weeded plots (Burke, 2008; Burke et al., 2011; Cantor et al., 2011), which has altered

186 the AM fungal community composition between treatments (Bialic-Murphy et al., 2021) (Table
187 1). These patterns have been observed despite evidence that soil nutrient availaiblity and soil
188 water availability does not differ between *A. petiolata* treatments (Bialic-Murphy et al., 2021;
189 Burke et al., 2019) (Table 1).
190

191 **Table 1** Summary of previous results at the Trillium Trail *A. petiolata* manipulation experiment

Metric Category	Metric	*A. petiolata* effect	Evidence	Citation
Soil characteristics	Soil moisture	No change	No difference between *A. petiolata*-ambient and weeded plots	(Bialic-Murphy et al., 2021; Burke et al., 2019)
	Soil nutrient availability	No change	No difference between *A. petiolata*-ambient and weeded plots	(Bialic-Murphy et al., 2021; Burke et al., 2019)
	Soil carbon	+	Soil C is greater in *A. petiolata*-weeded plots	(Burke et al., 2019)
AM fungal community composition and function	AM fungal spore germination	-	Reduced spore germination by *A. petiolata* allelochemicals	(Cantor et al., 2011)
	AM fungal colonization in roots	-	Higher colonization in *A. petiolata*-weeded treatment	(Mutz et al. in review; Bialic-Murphy et al., 2021)
	Soil AM fungal hyphal lengths	-	Lower fungal hyphal lengths in *A. petiolata*-ambient plots	(Cantor et al., 2011; Hale et al., 2016)
	AM fungal spore abundance in soil	No change	No change	(Burke et al., 2019)
	AM fungal diversity (richness) in soil	No change	No change	(Bialic-Murphy et al., 2021)
	AM fungal diversity (richness) in roots	No change	No change	(Mutz et al. in review)
	AM fungal community composition in soil	Change	Shifts in AM fungal composition in mineral soil	(Bialic-Murphy et al., 2021; Burke, 2008; Burke et al., 2011, 2019)
	AM fungal community composition in native plant roots	Change	Shifts in AM fungal composition in native plant roots	(Mutz et al. in review)
	Soil nutrient provisioning to native plants ($d^{15}N$)	-	Native plant $d^{15}N$ higher in *A. petiolata*-invaded plots	(Mutz et al. in review)
Native plant community structure	Mycorrhizal plant abundance	-	Abundance of native AM-associating plants decrease with *A. petiolata*	(Roche et al., 2021, 2023)
Physiology and allocation	Stored carbon (inulin) in *Maianthemum*	-	*A. petiolata* leaf litter reduced stored carbon (inulin) in *Maianthemum*	(Hale et al., 2016)
	Soil respiration (microbial activity)	-	*A. petiolata* tissue slowed soil respiration	(Hale et al., 2011)
	Net photosynthesis in *Maianthemum*	-	*A. petiolata* decreases net photosynthesis rates	(Brouwer et al., 2015; Hale et al., 2011)
	Stomatal conductance in *Maianthemum*	-	*A. petiolata* decreases stomatal conductance	(Brouwer et al., 2015; Hale et al., 2011)

Gas exchange measurements and calculations

Gas exchange measurements were collected between April and June 2023 from fully expanded leaves of two perennial understory native species: *Trillium* spp. (*Trillium grandiflorum* (Michx.) Salisb and *Trillium erectum* L.) and *Maianthemum racemosum* L. Link. We use *Trillium* spp. to refer to *T. grandiflorum* and *T. erectum*, as these species are difficult to distinguish if they are not reproductive. *Trillium* spp. and *M. racemosum* are each understory perennial herbs with widespread distributions in temperate forests of North America (USDA NRCS, 2022), form rhizomes, and associate with AM fungi (Brundrett & Kendrick, 1987, 1990; Burke, 2008). Previous work indicates that the timing of aboveground phenology differs between the two species: *Trillium* spp. typically emerge in late April and senesce in July, while *M. racemosum* typically emerge in early May and senesce as late as November (Heberling et al., 2019)

Gas exchange data were collected in three of the five experimental plots during two measurement periods: once early in the growth season when the tree canopy was open and tree canopy leaf out was occurring (April 19 through April 21 for *Trillium* spp. and May 5 through May 6 for *M. racemosum*) and once later in the growth season when the tree canopy was fully closed (June 12 through June 15 for both species). The remaining two plots were excluded from gas exchange measurements due to insufficient species replication in one plot and unforeseen field constraints in the other. Nonetheless, gas exchange data were collected in enough individuals across the sampled plots to confidently assess the effects of *A. petiolata* on native plant physiology (Table 2). The first measurement period was conducted at different time points for *Trillium* spp. and *M. racemosum* because of differences in the timing of full leaf expansion between species (Heberling et al., 2019).

Net photosynthesis (A_{net}; μmol m^{-2} s^{-1}), stomatal conductance (g_{sw}; mol m^{-2} s^{-1}), and intercellular CO_2 (C_i; μmol mol^{-1}) concentrations were measured across a range of atmospheric CO_2 concentrations (i.e., an A_{net}/C_i curve) using the Dynamic Assimilation™ Technique (Saathoff & Welles, 2021). This technique allows for high-throughput A_{net}/C_i curves that correspond well with traditional steady-state methods in herbaceous species (Tejera-Nieves et al., 2024). We generated all A_{net}/C_i curves along a reference CO_2 ramp down from 420 μmol mol^{-1} CO_2 to 20 μmol mol^{-1} CO_2, followed by a ramp up from 420 μmol mol^{-1} CO_2 to 1620 μmol mol^{-1} CO_2 after a 90-second wait period at 420 μmol mol^{-1} CO_2. The ramp rate for each curve was set to 200 μmol mol^{-1} min^{-1}, logging every five seconds, which generated 96 data points per

response curve. All A_{net}/C_i curves were initiated after A_{net} and g_{sw} stabilized in a LI-6800 cuvette set to a 500 mol s^{-1} flow rate, 10000 rpm mixing fan speed, 1.5 kPa vapor pressure deficit, 25°C leaf temperature, 2000 µmol m^{-2} s^{-1} incoming light radiation, and initial reference CO_2 set to 420 µmol mol^{-1}. We extracted snapshot A_{net} and g_{sw} measurements using the initial measurement of each A_{net}/C_i curve at 420 µmol mol^{-1} CO_2.

A/Ci curve fitting and parameter estimation

We fit A_{net}/C_i curves using the 'fitaci' function in the 'plantecophys' R package (Duursma, 2015). This function estimates the maximum rate of Rubisco carboxylation (V_{cmax}; µmol m^{-2} s^{-1}) and maximum rate of electron transport for RuBP regeneration (J_{max}; µmol m^{-2} s^{-1}) using the Farquhar et al. (1980) biochemical model of C_3 photosynthesis. Triose phosphate utilization (TPU) limitation was included as an additional rate-limiting step in all curve fits and the temperature standardization default in the function was turned off. Dark respiration was estimated in each curve fit as a fixed proportion of V_{cmax}. Michaelis-Menten coefficients for Rubisco affinity to CO_2 (K_c; µmol mol^{-1}) and O_2 (K_o; mmol mol^{-1}), and the CO_2 compensation point (Γ^*; µmol mol^{-1}) were calculated using leaf temperature and equations derived in Bernacchi et al. (2001):

$$K_c = 404.9 * exp^{\left(\frac{79430(T_k-298)}{298RT_k}\right)} \quad (1)$$

$$K_o = 278.4 * exp^{\left(\frac{36380(T_k-298)}{298RT_k}\right)} \quad (2)$$

$$\Gamma^* = 42.75 * exp^{\left(\frac{37830(T_k-298)}{298RT_k}\right)} \quad (3)$$

In all three equations, T_k is the mean leaf temperature (in Kelvin) during each A_{net}/C_i curve, and R is the universal gas constant (8.314 J mol^{-1} K^{-1}). All curves were visually inspected for goodness-of-fit before extracting V_{cmax} and J_{max} estimates for hypothesis testing.

For all A_{net}/C_i curve fits, V_{cmax} and J_{max} were standardized to 25°C (referenced as V_{cmax25} and J_{max25} from this point forward) using a modified Arrhenius equation. This temperature standardization removed the influence of enzyme kinetics on V_{cmax} and J_{max}, and, thus, reflected biochemical investment in the different underlying processes (Atkin & Tjoelker, 2003). Rate estimates were standardized to 25°C using the formulation presented in Kattge and Knorr (2007):

$$k_{25} = \frac{k_{obs}}{e^{\left[\frac{Ha(T_{obs}-T_{ref})}{T_{ref}RT_{obs}}\right]} \times \frac{1+e^{\left(\frac{T_{ref}\Delta S - H_d}{T_{ref}}\right)}}{1+e^{\left(\frac{T_{obs}\Delta S - H_d}{T_{obs}}\right)}}} \quad (4)$$

where k_{25} represents the standardized V_{cmax} or J_{max} rate at 25°C, k_{obs} represents the V_{cmax} or J_{max} estimate at the average leaf temperature measured inside the cuvette during the A_{net}/C_i curve. H_a is the activation energy of V_{cmax} (71,513 J mol^{-1}; Kattge and Knorr, 2007) or J_{max} (49,884 J mol^{-1}; Kattge and Knorr, 2007). H_d represents the deactivation energy of both V_{cmax} and J_{max} (200,000 J mol^{-1}; Medlyn et al., 2002), and R represents the universal gas constant (8.314 J mol^{-1} K^{-1}). T_{ref} represents the standardized temperature of 298.15 K, and T_{obs} represents the mean leaf temperature (K) during each A_{net}/C_i curve. ΔS is an entropy term (J mol^{-1} °C^{-1}) that Kattge and Knorr (2007) described as a linear relationship with acclimated growth temperature (T_g, °C), where:

$$\Delta S_{vcmax} = -1.07T_g + 668.39 \quad (5)$$

and:

$$\Delta S_{jmax} = -0.75T_g + 659.70 \quad (6)$$

We estimated T_g as the mean temperature of the seven days leading up to each A_{net}/C_i curve, following that photosynthetic acclimation typically occurs along this timescale (e.g., as found in Smith and Dukes, 2018). Mean daily air temperature was estimated using data collected at a nearby weather station (station ID: USW000114762; coordinates: 40.355° N, 79.921° W) included in the Global Historical Climatology Network - Daily data product (Menne et al., 2012). V_{cmax25} and J_{max25} estimates were used to calculate the ratio of J_{max25} to V_{cmax25} (J_{max25}:V_{cmax25}; unitless).

Stomatal limitation

The extent by which stomatal conductance limited net photosynthesis (unitless) was calculated following the approach described in Farquhar and Sharkey (1982), where:

$$Stomatal\ limitation = 1 - \frac{A_{net}}{A_{mod}} \quad (7)$$

A_{net} represents the measured net photosynthesis rate where atmospheric CO_2 is 420 μmol mol^{-1}. A_{mod} represents the theoretical photosynthetic rate where $C_i = C_a = 420$ μmol mol^{-1} (that is, no stomatal resistance to gas exchange), calculated as:

$$A_{mod} = V_{cmax}\frac{C_{i,mod}-\Gamma^*}{C_{i,mod}+K_m} - R_d \quad (8)$$

where V_{cmax} is the measured maximum rate of Rubisco carboxylation (i.e., not temperature-standardized to 25°C), $C_{i,mod}$ is the intercellular CO_2 concentration where $C_i = C_a$, set to 420 μmol mol^{-1}, Γ^* (μmol mol^{-1}) is the CO_2 compensation point in the absence of dark respiration, K_m is the Michaelis-Menten coefficient for Rubisco-limited photosynthesis (μmol mol^{-1}), and R_d is the dark respiration rate, estimated as a fixed proportion of V_{cmax}. K_m was calculated as:

$$K_m = K_c * \left(1 + \frac{O_i}{K_o}\right) \quad (9)$$

where K_c and K_o were calculated following Eqns. 1 and 2, respectively, while O_i is the leaf intercellular O_2 concentration, set to 210 μmol mol^{-1}.

Chlorophyll fluorescence measurements

Relative chlorophyll content was measured after each A_{net}/C_i curve on the same leaf using a Soil Plant Analysis Development chlorophyll meter (SPAD, unitless) built into the MultispeQ V2.0 handheld device (PhotosynQ Inc., East Lansing, MI, USA).

Soil characteristics

To characterize plant-available nitrogen and phosphorus at the time of leaf gas exchange measurements, resin strips (Membranes International Inc., Ringwood, NJ, USA) were placed approximately 10 cm below the soil surface to quantify mobile ammonium (ppm), nitrate (ppm), and phosphate (ppm) concentrations in each plot. An initial batch of resin strips was incubated in the field between April 19 and June 1, 2023, followed by a second batch inserted in the same plot location between May 30 and June 29, 2023. A total of 36 strips, 12 for each nutrient, were placed in each plot to account for the high degree of spatial heterogeneity of soil nutrient availability in temperate forests (Akana et al., 2023). Cation and anion concentrations were extracted from resin strips in 0.5 M potassium sulfate at a 1:5 dilution factor for ammonium, and nitrate, and 1 M HCl for phosphate. Concentrations of each nutrient were determined through end products of standard colorimetric reactions (D'Angelo et al., 2001; Doane & Horwáth, 2003; Lajtha et al., 1999; Weatherburn, 1967). Soil inorganic nitrogen availability was estimated as the sum of the ammonium and nitrate concentrations. The soil inorganic nitrogen-to-phosphorus

ratio was estimated as the ratio of soil inorganic nitrogen availability to soil phosphate availability.

Soil moisture data were collected using TOMST® TMS-4 data loggers (TOMST® s.r.o., Prague, Czech Republic). One data logger was placed in each *A. petiolata* treatment of each plot (i.e., 2 data loggers per plot) on April 26, 2023 and recorded soil moisture pulses every 15 minutes. Volumetric soil moisture content (%) was calculated using the calibration curves for a silt loam soil reported in Wild et al. (2019). We calculated the mean daily volumetric soil moisture content and used these values as the primary indicator of soil moisture throughout the measurement period.

319 **Table 2** Replication statement for levels of inference used in this study

Measurement type	Scale of Inference	Scale at which the factor of interest is applied	Number of replicates at the appropriate scale
Soil nutrient availability	Plot	Plot (treatment is imposed in split-plot design)	3 plots x 6 resin strips per nutrient type per *A. petiolata* treatment per plot (12 resin strips per nutrient type per plot) = 18 replicates per nutrient type per *A. petiolata* treatment (36 total resin strips per nutrient across plots)
Soil moisture	Plot	Plot (treatment is imposed in split-plot design)	3 plots x 1 soil moisture senser per *A. petiolata* treatment (2 soil moisture sensors per plot) = 3 replicates per *A. petiolata* treatment
Native plant photosynthetic traits	Species	7 photosynthetic traits per individual	4-22 individuals per species per *A. petiolata* treatment per plot. Total number of individuals per species: 78 *Trillium* spp. individuals, 68 *M. racemosum* individuals

320

321

Data analysis

We built a series of linear mixed-effects models to explore the effects of *A. petiolata* treatment and measurement period on soil nutrient availability. Each model included *A. petiolata* treatment (ambient, weeded) and measurement period (open, closed tree canopy) as fixed effects, with an additional interaction term between *A. petiolata* treatment and measurement period. Plot was included as a random intercept term. We constructed separate models with this independent variable structure for soil nitrate availability, soil ammonium availability, soil inorganic nitrogen (nitrate + ammonium) availability, soil phosphate availability, and the soil nitrogen-to-phosphorus ratio. The models for soil inorganic nitrogen availability and the soil nitrogen-to-phosphorus ratio were fitted using dependent variables that were natural-log transformed, while the model for soil ammonium availability was fitted after soil ammonium availability was square root-transformed to normalize model residuals (Shapiro-Wilk: $p>0.05$ in all cases).

Next, we built a linear mixed-effects model to explore the effect of *A. petiolata* treatment on volumetric soil moisture content across the measurement period. This model included *A. petiolata* treatment (ambient levels, weeded) and day of year (continuous) as fixed effects, with an added interaction term between *A. petiolata* treatment and day of year. Plot was included as a random intercept term.

Finally, we built a series of species-specific linear mixed-effects models to explore the effect of *A. petiolata* treatment and measurement period on leaf physiological traits of *Trillium* spp. and *M. racemosum*. Species were not concatenated into a single linear mixed-effect model for each trait because we did not seek to understand interspecies variability in measured traits. All models included *A. petiolata* treatment (ambient, weeded) and measurement period (open, closed tree canopy) as fixed effects, as well as an interaction term between *A. petiolata* treatment and measurement period. Plot was included as a random intercept term. We constructed separate models with this independent variable structure for each species for the following dependent variables: A_{net}, g_{sw}, stomatal limitation, V_{cmax25}, J_{max25}, J_{max25}:V_{cmax25}, and SPAD. Models for A_{net}, g_{sw}, V_{cmax25}, and J_{max25} in *Trillium* spp. were fitted using dependent variables that were natural-log transformed to normalize model residuals, while models for stomatal limitation, *SPAD*, and J_{max25} in *M. racemosum* were fitted using dependent variables that were natural-log transformed to normalize model residuals (Shapiro-Wilk: $p>0.05$ in all cases).

Each model was fitted using the 'lmer' function in the 'lme4' R package (Bates *et al.*, 2015). Type II Wald's χ^2 and the significance (α=0.05) of each fixed effect coefficient was calculated using the 'Anova' function in the 'car' R package (Fox & Weisberg, 2019). We used the 'emmeans' R package (Lenth, 2019) to conduct post hoc comparisons using Tukey's tests, where degrees of freedom were approximated using the Kenward-Roger approach (Kenward & Roger, 1997). All analyses and plots were conducted in R version 4.1.0 (R Core Team, 2021). Data, analysis scripts, and plot scripts are available on Zenodo (DOI: 10.5281/13862911).

Results

Soil characteristics

Soil inorganic nitrogen availability was reduced by 75% (p<0.001, Table S1; Fig. 1a) and soil phosphate availability was reduced by 26% (p<0.001, Table S1; Fig. 1b) after tree canopy closure, leading to 63% decrease in the soil nitrogen-to-phosphorus ratio (p<0.001, Table S1; Fig. 1c). Soil nitrate availability decreased by 71% after the tree canopy closed (p<0.001, Table S1; Fig. S1), whereas soil ammonium availability did not change between measurement periods (p=0.255, Table S1; Fig. S1).

Alliaria petiolata treatment had no effect on soil inorganic nitrogen availability (p=0.371, Table S1; Fig. 1a), soil phosphate availability (p=0.108, Table S1; Fig. 1b), soil ammonium availability (p=0.370, Table S1; Fig. S1), or soil nitrate availability (p=0.106, Table S1; Fig. S1). However, the soil nitrogen-to-phosphorus ratio was 51% greater in the *A. petiolata*-ambient treatment compared to the *A. petiolata*-weeded treatment (p=0.038, Table S1; Fig. 1c) due to an insignificant 16% increase in soil inorganic nitrogen availability (p=0.370, Table S1) and insignificant 15% decrease in soil phosphate availability (p=0.106, Table S1; Fig. 1b) in the *A. petiolata*-ambient treatment compared to the *A. petiolata*-weeded treatment.

Soil moisture decreased as the growth season progressed (p<0.001; Table S2; Fig. 2) and was lower in the *A. petiolata*-ambient treatment than the *A. petiolata*-weeded treatment (p<0.001; Table S1).

379 **Figure 1**

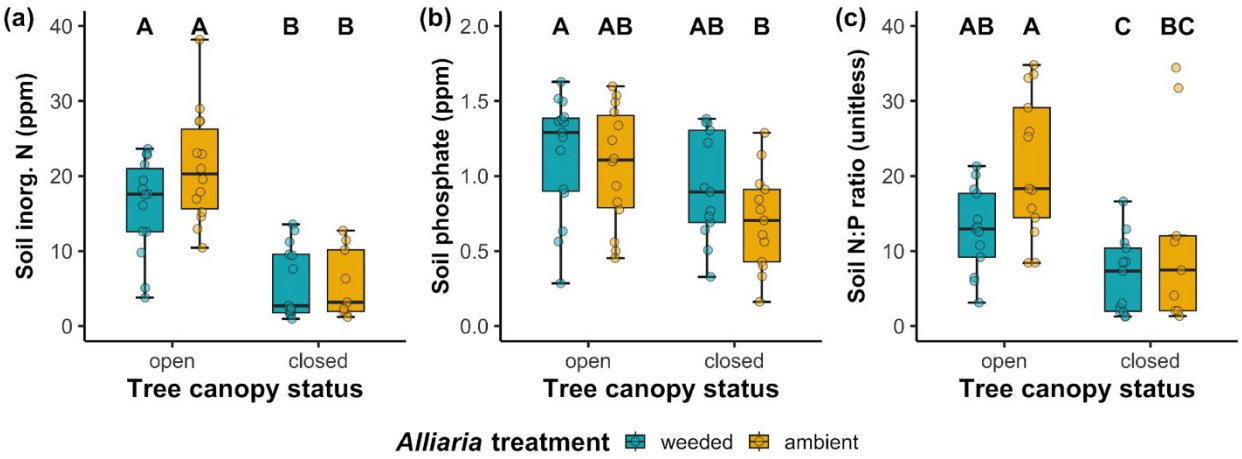

380

381 **Figure 1** Effects of tree canopy and *A. petiolata* treatment on soil inorganic nitrogen availability
382 (a), soil phosphate availability (b), and the soil nitrogen: phosphorus ratio (c). Tree canopy status
383 is on the x-axis. Teal points and boxplots indicate measurements collected in plots where *A.*
384 *petiolata* was weeded and gold points and boxplots indicate measurements collected in subplots
385 where *A. petiolata* was present at ambient levels. Boxes represent the upper (75% percentile) and
386 lower (25% percentile) quartiles, and whiskers represent 1.5 times the upper and lower quartile
387 values. Lettering above each treatment group indicates statistically different groups where
388 Tukey: $p<0.05$.

389

Figure 2

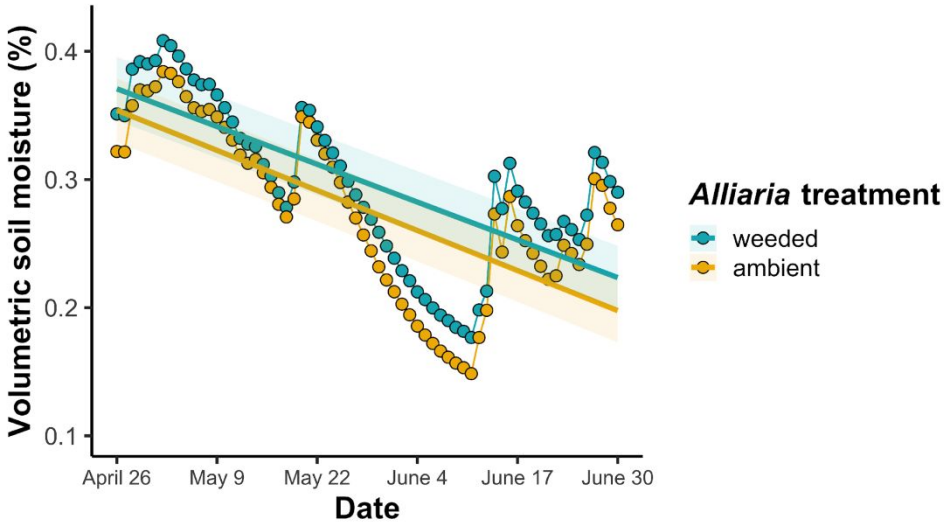

Figure 2 Effects of *A. petiolata* treatment on mean daily volumetric soil moisture content across the 2023 growth season. Date is on the x-axis. Points reference daily volumetric soil water content averaged across the three plots used to collect gas exchange measurements. The teal points and trendline indicate measurements collected in plots where *A. petiolata* was weeded and gold points and trendline indicate measurements collected in plots where *A. petiolata* was present at ambient levels. Error ribbons represent the trendline standard error.

Gas exchange

For *Trillium* spp., net photosynthesis decreased by 64% after tree canopy closure (p<0.001, Table 3; Fig. 3a), a pattern that was associated with a 22% reduction in stomatal conductance (p<0.001, Table 3; Fig. 3c) and 55% reduction in stomatal limitation (p<0.001, Table 3; Fig. 3e) compared to measurements collected before tree canopy closure. Net photosynthesis rates were reduced in the *A. petiolata*-ambient treatment compared to the *A. petiolata*-weeded treatment (p=0.016, Table 3; Fig. 3a). However, this net photosynthesis response to *A. petiolata* treatment was only observed after tree canopy closure (*A. petiolata* treatment-by-canopy status interaction: p=0.028, Table 3; Fig. 3a). *Alliaria petiolata* treatment had no effect on stomatal conductance (p=0.701, Table 3; Fig. 3c) or stomatal limitation (p=0.481, Table 3; Fig. 3e).

For *M. racemosum*, net photosynthesis decreased by 59% after tree canopy closure (p<0.001, Table 3; Fig. 3b), a pattern that was associated with a 62% reduction in stomatal conductance (p<0.001, Table 3; Fig. 3d) and a 13% increase in stomatal limitation (p=0.004, Table 3; Fig. 3f) compared to measurements collected before tree canopy closure. Net photosynthesis decreased by 18% (p<0.001, Table 3) and stomatal conductance decreased by 27% (p<0.001, Table3), while stomatal limitation increased by 28% (p<0.001, Table 3) in the *A. petiolata*-ambient treatment compared to the *A. petiolata*-weeded treatment. Net photosynthesis and stomatal conductance responses to *A. petiolata* treatment were observed regardless of measurement period (*A. petiolata* treatment-by-canopy status interaction: p>0.05 in both cases, Table 3), while stomatal limitation responses to *A. petiolata* treatment were only observed after tree canopy closure (*A. petiolata* treatment-by-canopy status interaction: p=0.024, Table 3; Fig. 3f).

Relative chlorophyll content

SPAD values were 26% greater in *Trillium* spp. (p<0.001, Table 3; Fig. S2) and 51% greater in *M. racemosum* (p<0.001, Tablev3; Fig. S2) after tree canopy closure compared to before tree canopy closure. *A. petiolata* treatment had no effect on SPAD in either species (p>0.05 in both cases, Table 3).

Table 3 Analysis of variance results for the effects of *A. petiolata* treatment and measurement period on leaf gas exchange*

	A_{net}		g_{sw}		Stomatal limitation		*SPAD*	
	χ^2	*p*	χ^2	*p*	χ^2	*p*	χ^2	*p*
***Trillium* spp.**								
A. petiolata treatment (A)	5.830	**0.016**	0.148	0.701	0.498	0.481	0.300	0.584
Canopy status (C)	1163.336	**<0.001**	23.864	**<0.001**	289.318	**<0.001**	73.833	**<0.001**
A*C	4.833	**0.028**	0.622	0.430	0.132	0.717	0.496	0.481
M. racemosum								
A. petiolata treatment (A)	19.547	**<0.001**	20.507	**<0.001**	15.684	**<0.001**	1.792	0.181
Canopy status (C)	336.988	**<0.001**	157.676	**<0.001**	8.300	**0.004**	285.711	**<0.001**
A*C	0.012	0.913	0.046	0.831	5.094	**0.024**	0.853	0.356

*Significance determined using Type II Wald χ^2 tests (α=0.05). *P*-values less than 0.05 are in bold. Key: A_{net} = light-saturated net photosynthesis rate (μmol m^{-2} s^{-1}), g_{sw} = stomatal conductance (mol m^{-2} s^{-1}), SPAD = relative chlorophyll content (unitless)

Figure 3

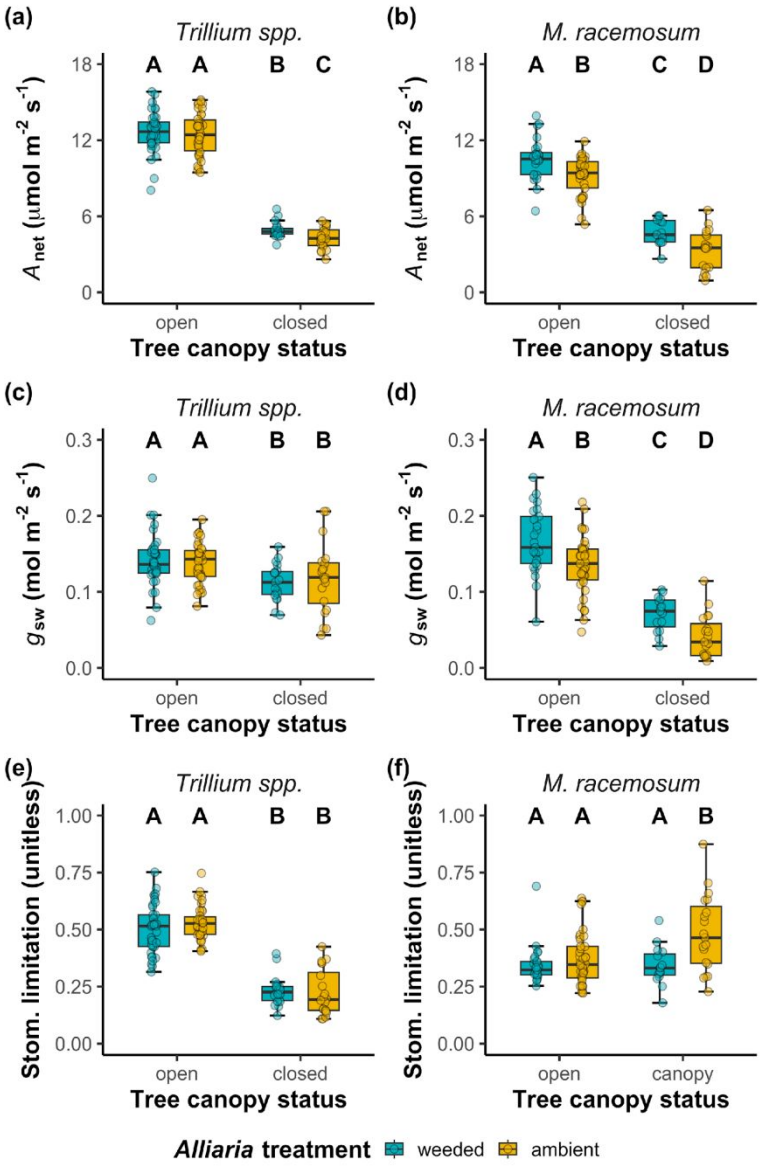

Figure 3 Effects of *A. petiolata* treatment and tree canopy status on net photosynthesis (A_{net}, a-b), stomatal conductance (g_{sw}, c-d), and stomatal limitation of net photosynthesis (e-f). The left column shows *Trillium* spp. responses, while the right column shows *M. racemosum* responses. Tree canopy status is on the x-axis. Teal points and boxplots indicate measurements collected in plots where *A. petiolata* was weeded and gold points and boxplots indicate measurements collected in plots where *A. petiolata* abundance was not manipulated. Boxes represent the upper (75% percentile) and lower (25% percentile) quartiles, and whiskers represent 1.5 times the upper and lower quartile values. Lettering above each treatment group indicates statistically different groups where Tukey: $p<0.05$.

443 *Photosynthetic capacity*

444 In *Trillium* spp., V_{cmax25} decreased by 76% (p<0.001, Table 4; Fig. 4a) and J_{max25} decreased by
445 75% (p<0.001, Table 4; Fig. 4c) following tree canopy closure. These patterns resulted in a 4%
446 increase in J_{max25}:V_{cmax25} after tree canopy closure compared to before tree canopy closure
447 (p=0.007; Table 4; Fig. 4e). *Alliaria petiolata* treatment had no effect on V_{cmax25} (p=0.296; Table
448 4; Fig. 4a) or J_{max25}:V_{cmax25} (p=0.386, Table 4; Fig. 4e). However, J_{max25} was reduced by 8% in
449 the *A. petiolata*-ambient treatment compared to the *A. petiolata*-weeded treatment (p=0.045;
450 Table 4; Fig. 4c), a pattern that was only observed after tree canopy closure (*A. petiolata*
451 treatment-by-canopy status interaction: p=0.020; Table 4; Fig. 4c).

452 For *M. racemosum*, V_{cmax25} (p<0.001, Table 4; Fig. 4b) and J_{max25} (p<0.001, Table 4; Fig.
453 4d) each decreased by 57% after tree canopy closure compared to before tree canopy closure,
454 while J_{max25}:V_{cmax25} decreased by 5% (p=0.004, Table 4; Fig. 4f). The decrease in J_{max25}:V_{cmax25}
455 due to tree canopy closure was only observed in the *A. petiolata*-weeded treatment (*A. petiolata*
456 treatment-by-canopy status interaction: p=0.073; Table 4; Fig. 4f). *Alliaria petiolata* treatment
457 had no effect on V_{cmax25} (p=0.688, Table 4) , J_{max25} (p=0.543, Table 4), or J_{max25}:V_{cmax25} (p=0.113,
458 Table 4).

459

460 **Table 4** Analysis of variance results for the effects of *A. petiolata* treatment and measurement
461 period on apparent photosynthetic capacity*

	V_{cmax25}		J_{max25}		J_{max25}:V_{cmax25}	
	χ^2	*p*	χ^2	*p*	χ^2	*p*
***Trillium* spp.**						
A. petiolata treatment (A)	1.090	0.296	4.008	**0.045**	2.622	0.105
Canopy status (C)	1585.012	**<0.001**	2001.653	**<0.001**	7.314	**0.007**
A*C	1.973	0.160	5.417	**0.020**	0.753	0.386
M. racemosum						
A. petiolata treatment (A)	0.162	0.688	0.370	0.543	2.510	0.113
Canopy status (C)	284.148	**<0.001**	391.314	**<0.001**	8.456	**0.004**
A*C	0.219	0.640	0.045	0.832	3.221	*0.073*

462 *Significance determined using Type II Wald χ^2 tests (α=0.05). *P*-values less than 0.05 are in
463 bold, while values where $0.05<p<0.1$ are italicized. Key: V_{cmax25} = maximum rate of Rubisco
464 carboxylation at 25°C (μmol m^{-2} s^{-1}), J_{max25} = maximum rate of electron transport for RuBP
465 regeneration at 25°C (μmol m^{-2} s^{-1}), J_{max25}:V_{cmax25} = ratio of J_{max25} to V_{cmax25} (unitless)
466

Figure 4

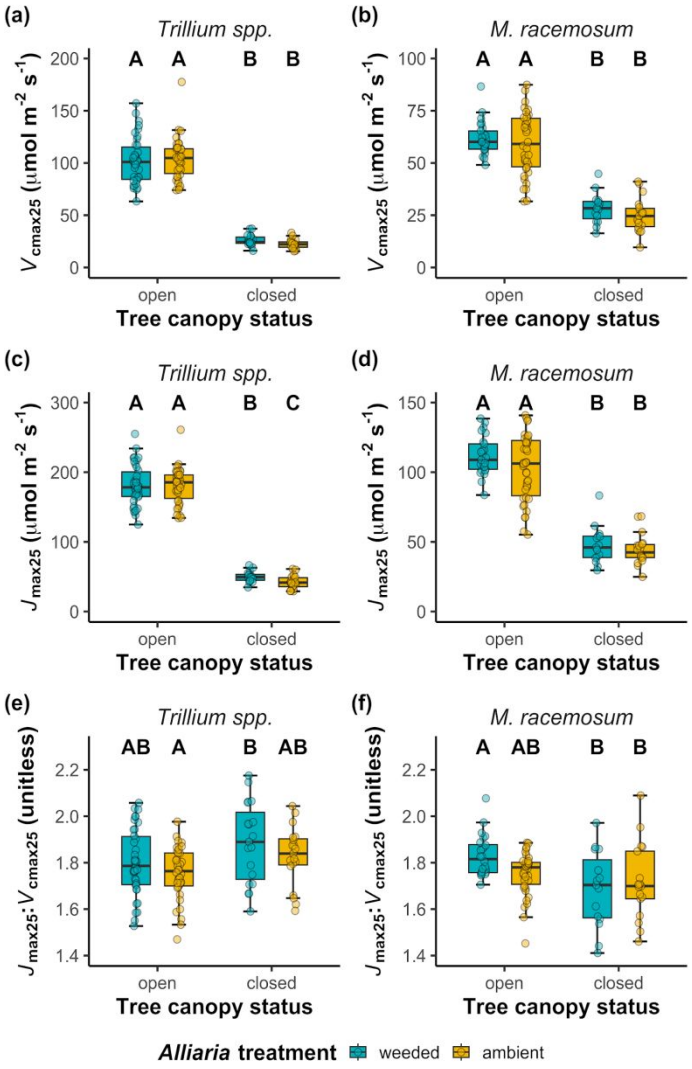

Figure 4 Effects of *A. petiolata* treatment and tree canopy status on the temperature-standardized maximum rate of Rubisco carboxylation (V_{cmax25}; a-b), the temperature-standardized maximum rate of electron transport for RuBP regeneration (J_{max25}; c-d), and the ratio J_{max25}:V_{cmax25} (e-f). The left column shows *Trillium* spp. responses, while the right column shows *M. racemosum* responses. Tree canopy status is on the x-axis. Teal points and boxplots indicate measurements collected in subplots where *A. petiolata* was weeded, and gold points and boxplots indicate measurements collected in subplots where *A. petiolata* abundance was not manipulated. Boxes represent the upper (75% percentile) and lower (25% percentile) quartiles, and whiskers represent 1.5 times the upper and lower quartile values. Lettering above each treatment group indicates statistically different groups where Tukey: $p<0.05$.

Discussion

Both native species growing under ambient levels of *A. petiolata* exhibited significantly reduced net photosynthesis rates compared to those growing in the *A. petiolata*-weeded treatment, supporting our first hypothesis. For *Trillium* spp., the net photosynthesis response to the *A. petiolata* treatment was associated with a reduction in apparent photosynthetic capacity, but no change in stomatal conductance and stomatal limitation. Conversely, the net photosynthesis response in *M. racemosum* to *A. petiolata* treatment was associated with a reduction in stomatal conductance that increased stomatal limitation and no change in apparent photosynthetic capacity. Building on results reported in Bialic-Murphy et al. (2021), these observations suggest that *A. petiolata* invasion modifies net photosynthesis rates by altering nutrient uptake and allocation to photosynthetic enzymes in *Trillium* spp. and by altering water uptake and use for photosynthesis in *M. racemosum*.

While the mechanisms that drove photosynthetic responses to *A. petiolata* treatment were different between the two species, native plant responses to *A. petiolata* treatment were generally more pronounced late after tree canopy closure for both species. This pattern negated our second hypothesis that the negative effects of allelopathic plant invasion would be greatest early in the season when understory demand for soil resources is greatest, although supported our alternative hypothesis that these effects would be strongest later in the growth season when soil resources were depleted. Indeed, stronger late-season photosynthetic responses to ambient levels of *A. petiolata* coincided with a reduction in soil nutrient availability and soil moisture as the growing season progressed, which may have increased reliance on AM fungal partners for soil resources (Kummel & Salant, 2006; Treseder, 2004; van Diepen et al., 2007). Disruptions in AM fungal mutualism function due to the allelopathic invader may have increased the cost of acquiring soil resources, potentially altering resource uptake and allocation to photosynthetic tissues (Waring et al., 2023). These patterns may have been exacerbated by the reduction in soil moisture in the *A. petiolata*-ambient treatment compared to the *A. petiolata*-weeded treatment, which may have further increased late-season reliance on disrupted AM fungal partners for soil resources in the *A. petiolata*-ambient treatment.

Overall, our results indicate that native plant responses to the allelopathic invader intensified as the growth season progressed, even though the mechanisms that drove individual species responses differed. These findings provide important insight into understanding native

plant responses to allelopathic plant invasion and highlight the need to understand these responses through time. Understanding the temporal impacts of plant invasions will improve our ability to predict the consequences of plant invasion on native plant community dynamics, providing an important link for understanding how the effects of plant invasion on belowground soil microbial communities scale to impact aboveground plant population demography and community function.

Photosynthetic responses to A. petiolata presence are linked to altered nutrient and water economics

Net photosynthesis rates were reduced in the *A. petiolata*-ambient treatment for both *Trillium* spp. and *M. racemosum*, but the mechanisms underlying these responses differed between species. *Trillium* spp. responses to *A. petiolata* treatment suggest that the allelopathic invader induced a form of nutrient stress, modifying net photosynthesis by reducing apparent photosynthetic capacity through a likely shift in nutrient allocation to photosynthetic enzymes. The null effect of *A. petiolata* treatment on relative chlorophyll content and the temperature-standardized apparent maximum rate of Rubisco carboxylation (V_{cmax25}) coupled with a reduction in the temperature-standardized apparent maximum rate of electron transport for RuBP regeneration (J_{max25}) in the *A. petiolata*-ambient treatment implies that any reduction in nutrient provisioning toward photosynthetic enzymes may have been due to a reduction in the fraction of leaf nutrients allocated to bioenergetics (Niinemets et al., 1998; Niinemets & Tenhunen, 1997; Waring et al., 2023). Null effects of *A. petiolata* treatment on stomatal conductance and stomatal limitation indicate that *A. petiolata* does not impact the water economics of *Trillium* spp., suggesting that the physiological responses to the allelopathic invader were driven entirely by shifts in nutrient economics.

In contrast, *M. racemosum* responses to *A. petiolata* treatment suggest that presence of the allelopathic invader induced a form of water stress, as reduced net photosynthesis rates in the *A. petiolata*-ambient treatment were driven by a reduction in stomatal conductance that increased late-season stomatal limitation. While these effects could have been due to direct phytotoxic effects of *A. petiolata* on *M. racemosum* through reductions in soil moisture, similar net photosynthesis and stomatal conductance patterns were observed in a controlled greenhouse experiment under well-watered conditions (Hale et al., 2016). These patterns corresponded with

null effects of *A. petiolata* treatment on apparent photosynthetic capacity, supporting previous work suggesting that physiological responses of *M. racemosum* to *A. petiolata* invasion are associated with changes in water economics, not nutrient economics (Hale et al., 2011, 2016).

The differences in the physiological responses of *Trillium* spp. and *M. racemosum* may be due in part to differences in leaf economic strategy. While *Trillium* spp. and *M. racemosum* share many functional and ecological traits, such as forming rhizomes, reproducing clonally, acquiring nutrients and water through direct uptake pathways or symbioses with AM fungi, and emerging at similar times (Brundrett & Kendrick, 1987, 1990; Heberling et al., 2019), these two species differ in leaf lifespan, placing them at different positions along the leaf economics spectrum (Onoda et al., 2017; Reich, 2014; Wright et al., 2004). In *Trillium* spp., shorter leaf lifespans may require rapid nutrient and water uptake to allow for fast growth and reproduction, leading to high leaf nutrient demand to build and maintain photosynthetic enzymes. In contrast, longer leaf lifespans in *M. racemosum* may foster resource-conservative strategies that favor long-term investment in photosynthetic tissues with reduced leaf nutrient demand to build and maintain photosynthetic enzymes and greater water demands to support photosynthesis across a longer growing season. Indeed, *M. racemosum* had lower temperature-standardized maximum rates of Rubisco carboxylation than *Trillium* spp. on average (V_{cmax25} mean ± SD: 48.4 ± 19.6 μmol m^{-2} s^{-1} in *M. racemosum* compared to 76.4 ± 40.9 μmol m^{-2} s^{-1} in *Trillium* spp.), reflecting a more resource-conservative strategy compared to *Trillium* spp.

The greater resource demand for photosynthetic enzyme production and maintenance in *Trillium* spp. may explain why its photosynthetic capacity was reduced in the *A. petiolata*-ambient treatment, especially if individuals relied more heavily on disrupted AM fungi for nutrient uptake. In other words, disrupted AM fungal communities due to *A. petiolata* presence may have made it more difficult for *Trillium* spp. individuals to satisfy demand to build and maintain photosynthetic enzymes, inducing nutrient stress and reducing net photosynthesis rates despite *A. petiolata* having no direct effect on soil nutrient availability. In contrast, resource conservative strategies for *M. racemosum* may have allowed individuals to satisfy nutrient demand to build and maintain photosynthetic enzymes irrespective of whether individuals were associated with disrupted AM fungal partners. However, longer leaf lifespans may have increased demand for maintaining transpiration streams needed to support net photosynthesis across the growing season. If true, reduced soil moisture across the growing season paired with

increasingly reduced soil moisture in the *Alliaria*-ambient treatment may have caused individuals to no longer be able to satisfy demand for maintaining transpiration rates needed to maintain net photosynthesis. Isotopic tracer studies paired with water manipulation experiments may be useful for confirming these conjectures and would allow us to better understand the carbon-for-resource exchange that regulates plant-AM symbioses.

Photosynthetic responses to A. petiolata presence intensify as the growing season progresses

We hypothesized that the effects of *A. petiolata* treatment on leaf-level photosynthesis would be more apparent early in the growing season when understory demand for maintaining photosynthetic enzymes and a desired transpiration stream is greatest (Heberling et al., 2019). Contrary to this hypothesis, the effects of *A. petiolata* treatment were absent (for *Trillium* spp.) or relatively weak (for *M. racemosum*) before tree canopy closure. For *M. racemosum*, the early-season reduction in net photosynthesis and stomatal conductance was associated with lower soil moisture in the *A. petiolata*-ambient treatment compared to the *A. petiolata*-weeded treatment, which may have caused individuals to close stomata as a water-savings mechanism or rely more on disrupted AM fungal partners for water.

Limited early-season photosynthetic responses to *A. petiolata* treatment may be attributed to resource optimization that caused individuals to favor investment toward direct uptake regardless of *A. petiolata* treatment. Resource optimization theory predicts that, given multiple potential acquisition strategies (e.g., direct uptake, mycorrhizal symbioses, etc.), plants should prioritize investment toward the resource uptake strategy that minimizes the cost and maximizes the uptake efficiency of acquiring soil resources (Bloom et al., 1985; Kummel & Salant, 2006; Rastetter et al., 2001). Thus, plants should invest more strongly in direct uptake pathways early in the growing season when soil resources are more abundant, as costs to acquire soil resources through direct uptake pathways are often reduced under high resource availability (Lu et al., 2022; Perkowski et al., 2021, 2024). Therefore, limited photosynthetic responses to *A. petiolata* treatment early in the growing season may have been due to investment toward direct uptake that allowed individuals to satisfy demand to build and maintain photosynthetic enzymes and maintain transpiration while minimizing any negative consequence of relying on AM fungal partners for resources.

Alternatively, we hypothesized that the effects of *A. petiolata* treatment on leaf-level photosynthetic traits would intensify as the growing season progressed. Our findings support this hypothesis, as both native species exhibited stronger reductions in net photosynthesis rates under ambient levels of *A. petiolata* after tree canopy closure than before tree canopy closure. This pattern was associated with decreased nitrogen availability, phosphorus availability, and soil moisture following tree canopy closure. Late-season photosynthetic responses were observed despite *A. petiolata* treatment having no direct effect on nitrogen or phosphorus availability, although soil moisture was reduced, and the soil nitrogen-to-phosphorus ratio was increased in the *A. petiolata*-ambient treatment. These patterns suggest that late-season photosynthetic responses to *A. petiolata* treatment may have been due to increased reliance on disrupted AM fungal partners as the cost to acquire resources through direct uptake increased with reduced nutrient and water availability (Perkowski et al., 2021, 2024). This may have been further exacerbated by stronger soil moisture reductions in the *A. petiolata*-ambient treatment and may have also been indicative of increased phosphorus limitation. It is important to note that we did not explicitly assess the link between AM fungal mutualism disruption and native plant physiology responses to *A. petiolata*. However, the patterns observed here indicate that this is an important next step toward understanding how soil microbial community disruptions due to allelopathic invaders scales to impact native plant physiology and community composition. Specifically, future work involving isotopic tracers (e.g., Hodge & Fitter, 2010) or soil resource manipulation experiments that cross AM fungal community compositions (e.g., Gustafson & Casper, 2004) would be a useful next step for linking soil microbial community, soil resource availability, and photosynthetic responses to allelopathic invaders.

Overall, these findings highlight the necessity of quantifying the temporal effects of plant invasion on coexisting native plant populations. Ecophysiological studies have traditionally focused on assessing the impacts of allelopathic invaders on the physiological processes of coexisting native species at single timepoints. While data from these studies are useful for understanding snapshot effects of plant invasion on native population physiology, they risk providing misleading results when using these responses to understand consequences of plant invasion on native population and community dynamics. This risk may be especially important in dynamic systems where light availability is dependent on tree canopy establishment and soil resource availability declines across the growing season. Experiments that assess the impacts of

plant invasion across multiple timepoints, as shown here, provide important insight into understanding the temporal nuances that underpin the effects of plant invasion on native populations and provide important empirical data that will improve our ability to reliably predict the impacts of plant invasion on plant population and community dynamics. Furthermore, soil microbial and plant communities operate on largely different spatiotemporal scales, which poses a big challenge when scaling soil microbial dynamics up to plant community dynamics. Quantifying the temporal effects of plant invasion on coexisting native plant populations may allow us to better integrate and scale the effects of plant invasions on belowground soil microbial and plant community dynamics.

Using leaf physiology to assess linkages between aboveground and belowground responses to allelopathic plant invasion

Native species' physiological responses to *A. petiolata* treatments have direct implications for understanding the integrated negative effects of *A. petiolata* invasion on the belowground soil microbial community and aboveground plant community form and function. *Alliaria petiolata* disrupts the belowground AM fungal community composition by reducing AM fungal biomass and root colonization rates while increasing AM fungal richness (Anthony et al., 2019; Bialic-Murphy et al., 2021; Burke, 2008; Burke et al., 2011, 2019; Cantor et al., 2011; Roche et al., 2021). This allelopathic invader also negatively affects the abundance and survivorship of AM native plants that coexist with *A. petiolata* in its non-native range (Bialic-Murphy et al., 2020; Callaway et al., 2008; Roche et al., 2021, 2023). Our results indicate that photosynthetic responses to *A. petiolata* are directionally similar its impacts on AM fungal community and plant community dynamics, suggesting that the effects of *A. petiolata* invasion across these levels of organization may be inherently linked and scalable through its impacts on native plant physiology. In other words, disruptions in AM fungal community composition due to *A. petiolata* invasion modify nutrient and water provisioning and uptake in native plant species, which decreases net carbon assimilation and, over time, has negative consequences for plant community survivorship and fitness.

Conclusions

The *A. petiolata*-ambient treatment negatively affected leaf-level photosynthetic processes in two native AM fungal-associating understory perennial species. While these patterns were driven by species-specific mechanisms, the negative effects of *A. petiolata* presence were stronger in both species after the tree canopy closed and soil resource availability decreased. These patterns highlight the need to understand species-specific responses to allelopathic invasion and other anthropogenic stressors to native ecosystems, and to specifically consider the temporal scale by which these factors might modify native plant communities. Our results provide important insight into understanding the mechanisms that drive photosynthetic responses to allelopathic plant invasion and are a critical piece of empirical data needed to link the effects of allelopathic plant invasion on belowground soil microbial communities with its effects on plant population and community dynamics. Furthermore, these findings indicate that understanding the temporal effects of invasion on coexisting native species may be important for predicting the effects of invasion and other anthropogenic drivers of environmental change on population and community dynamics.

References

Akana, P. R., Mifsud, I. E. J., & Menge, D. N. L. (2023). Soil nitrogen availability in a temperate forest exhibits large variability at sub-tree spatial scales. *Biogeochemistry*, *164*(3), 537–553. https://doi.org/10.1007/s10533-023-01056-5

Anthony, M. A., Stinson, K. A., Trautwig, A. N., Coates-Connor, E., & Frey, S. D. (2019). Fungal communities do not recover after removing invasive *Alliaria petiolata* (garlic mustard). *Biological Invasions*, *21*(10), 3085–3099. https://doi.org/10.1007/s10530-019-02031-8

Atkin, O. K., & Tjoelker, M. G. (2003). Thermal acclimation and the dynamic response of plant respiration to temperature. *Trends in Plant Science*, *8*(7), 343–351. https://doi.org/10.1016/S1360-1385(03)00136-5

Bernacchi, C. J., Singsaas, E. L., Pimentel, C., Portis, A. R., & Long, S. P. (2001). Improved temperature response functions for models of Rubisco-limited photosynthesis. *Plant, Cell and Environment*, *24*(2), 253–259. https://doi.org/10.1046/j.1365-3040.2001.00668.x

692 Bialic-Murphy, L., Brouwer, N. L., & Kalisz, S. (2020). Direct effects of a non-native invader
693 erode native plant fitness in the forest understory. *Journal of Ecology*, *108*(1), 189–198.
694 https://doi.org/10.1111/1365-2745.13233
695 Bialic-Murphy, L., Smith, N. G., Voothuluru, P., McElderry, R. M., Roche, M. D., Cassidy, S.
696 T., Kivlin, S. N., & Kalisz, S. (2021). Invasion-induced root–fungal disruptions alter plant
697 water and nitrogen economies. *Ecology Letters*, *24*(6), 1145–1156.
698 https://doi.org/10.1111/ele.13724
699 Bloom, A. J., Chapin, F. S., & Mooney, H. A. (1985). Resource limitation in plants-an economic
700 analogy. *Annual Review of Ecology and Systematics*, *16*(1), 363–392.
701 https://doi.org/10.1146/annurev.es.16.110185.002051
702 Brouwer, N. L., Hale, A. N., & Kalisz, S. (2015). Mutualism-disrupting allelopathic invader
703 drives carbon stress and vital rate decline in a forest perennial herb. *AoB PLANTS*, *7*(1), 1–
704 14. https://doi.org/10.1093/aobpla/plv014
705 Brundrett, M. C., & Kendrick, B. (1987). The mycorrhizal status, root anatomy, and phenology
706 of plants in a sugar maple forest. *Canadian Journal of Botany*, *66*, 1153–1173.
707 Brundrett, M. C., & Kendrick, B. (1990). The roots and mycorrhizas of herbaceous woodland
708 plants: I. Quantitative aspects of morphology. *New Phytologist*, *114*(3), 457–468.
709 https://doi.org/10.1111/j.1469-8137.1990.tb00415.x
710 Burke, D. J. (2008). Effects of *Alliaria petiolata* (garlic mustard; Brassicaceae) on mycorrhizal
711 colonization and community structure in three herbaceous plants in a mixed deciduous
712 forest. *American Journal of Botany*, *95*(11), 1416–1425.
713 https://doi.org/10.3732/ajb.0800184
714 Burke, D. J., Carrino-Kyker, S. R., Hoke, A., Cassidy, S., Bialic-Murphy, L., & Kalisz, S.
715 (2019). Deer and invasive plant removal alters mycorrhizal fungal communities and soil
716 chemistry: Evidence from a long-term field experiment. *Soil Biology and Biochemistry*,
717 *128*(September 2018), 13–21. https://doi.org/10.1016/j.soilbio.2018.09.031
718 Burke, D. J., Weintraub, M. N., Hewins, C. R., & Kalisz, S. (2011). Relationship between soil
719 enzyme activities, nutrient cycling and soil fungal communities in a northern hardwood
720 forest. *Soil Biology and Biochemistry*, *43*(4), 795–803.
721 https://doi.org/10.1016/j.soilbio.2010.12.014

722 Callaway, R. M., Cipollini, D., Barto, K., Thelen, G. C., Hallett, S. G., Prati, D., Stinson, K., &
723 Klironomos, J. (2008). Novel weapons: Invasive plant suppresses fungal mutualists in
724 America but not in its native Europe. *Ecology*, *89*(4), 1043–1055.
725 https://doi.org/10.1890/07-0370.1
726 Callaway, R. M., & Ridenour, W. M. (2004). Novel weapons: Invasive success and the evolution
727 of increased competitive ability. *Frontiers in Ecology and the Environment*, *2*(8), 436–443.
728 https://doi.org/10.1890/1540-9295(2004)002[0436:NWISAT]2.0.CO;2
729 Cantor, A., Hale, A., Aaron, J., Traw, M. B., & Kalisz, S. (2011). Low allelochemical
730 concentrations detected in garlic mustard-invaded forest soils inhibit fungal growth and
731 AMF spore germination. *Biological Invasions*, *13*(12), 3015–3025.
732 https://doi.org/10.1007/s10530-011-9986-x
733 D'Angelo, E., Crutchfield, J., & Vandiviere, M. (2001). Rapid, sensitive, microscale
734 determination of phosphate in water and soil. *Journal of Environmental Quality*, *30*(6),
735 2206–2209. https://doi.org/10.2134/jeq2001.2206
736 Doane, T. A., & Horwáth, W. R. (2003). Spectrophotometric determination of nitrate with a
737 single reagent. *Analytical Letters*, *36*(12), 2713–2722. https://doi.org/10.1081/AL-
738 120024647
739 Dong, N., Prentice, I. C., Evans, B. J., Caddy-Retalic, S., Lowe, A. J., & Wright, I. J. (2017).
740 Leaf nitrogen from first principles: field evidence for adaptive variation with climate.
741 *Biogeosciences*, *14*(2), 481–495. https://doi.org/10.5194/bg-14-481-2017
742 Dong, N., Prentice, I. C., Wright, I. J., Evans, B. J., Togashi, H. F., Caddy-Retalic, S.,
743 McInerney, F. A., Sparrow, B., Leitch, E., & Lowe, A. J. (2020). Components of leaf-trait
744 variation along environmental gradients. *New Phytologist*, *228*(1), 82–94.
745 https://doi.org/10.1111/nph.16558
746 Dong, N., Prentice, I. C., Wright, I. J., Wang, H., Atkin, O. K., Bloomfield, K. J., Domingues, T.
747 F., Gleason, S. M., Maire, V., Onoda, Y., Poorter, H., & Smith, N. G. (2022). Leaf nitrogen
748 from the perspective of optimal plant function. *Journal of Ecology*, *110*(11), 2585–2602.
749 https://doi.org/10.1111/1365-2745.13967
750 Duursma, R. A. (2015). Plantecophys - an R package for analysing and modelling leaf gas
751 exchange data. *PLOS ONE*, *10*(11), e0143346.
752 https://doi.org/10.1371/journal.pone.0143346

753 Evans, J. R., & Clarke, V. C. (2019). The nitrogen cost of photosynthesis. *Journal of*
754 *Experimental Botany*, *70*(1), 7–15. https://doi.org/10.1093/jxb/ery366
755 Evans, J. R., & Seemann, J. R. (1989). The allocation of protein nitrogen in the photosynthetic
756 apparatus: costs, consequences, and control. *Photosynthesis*, *8*, 183–205.
757 Farquhar, G. D., & Sharkey, T. D. (1982). Stomatal conductance and photosynthesis. *Annual*
758 *Review of Plant Physiology*, *33*(1), 317–345.
759 https://doi.org/10.1146/annurev.pp.33.060182.001533
760 Farquhar, G. D., von Caemmerer, S., & Berry, J. A. (1980). A biochemical model of
761 photosynthetic CO_2 assimilation in leaves of C_3 species. *Planta*, *149*(1), 78–90.
762 https://doi.org/10.1007/BF00386231
763 Fox, J., & Weisberg, S. (2019). *An R companion to applied regression* (Third edit). Sage.
764 https://socialsciences.mcmaster.ca/jfox/Books/Companion/
765 Gustafson, D. J., & Casper, B. B. (2004). Nutrient addition affects AM fungal performance and
766 expression of plant/fungal feedback in three serpentine grasses. *Plant and Soil*, *259*(1–2), 9–
767 17. https://doi.org/10.1023/B:PLSO.0000020936.56786.a4
768 Hale, A. N., & Kalisz, S. (2012). Perspectives on allelopathic disruption of plant mutualisms: A
769 framework for individual- and population-level fitness consequences. *Plant Ecology*,
770 *213*(12), 1991–2006. https://doi.org/10.1007/s11258-012-0128-z
771 Hale, A. N., Lapointe, L., & Kalisz, S. (2016). Invader disruption of belowground plant
772 mutualisms reduces carbon acquisition and alters allocation patterns in a native forest herb.
773 *New Phytologist*, *209*(2), 542–549. https://doi.org/10.1111/nph.13709
774 Hale, A. N., Tonsor, S. J., & Kalisz, S. (2011). Testing the mutualism disruption hypothesis:
775 physiological mechanisms for invasion of intact perennial plant communities. *Ecosphere*,
776 *2*(10), art110. https://doi.org/10.1890/es11-00136.1
777 Heberling, J. M., Cassidy, S. T., Fridley, J. D., & Kalisz, S. (2019). Carbon gain phenologies of
778 spring-flowering perennials in a deciduous forest indicate a novel niche for a widespread
779 invader. *New Phytologist*, *221*(2), 778–788. https://doi.org/10.1111/nph.15404
780 Hodge, A., & Fitter, A. H. (2010). Substantial nitrogen acquisition by arbuscular mycorrhizal
781 fungi from organic material has implications for N cycling. *Proceedings of the National*
782 *Academy of Sciences*, *107*(31), 13754–13759.

783 Hungate, B. A., Dukes, J. S., Shaw, M. R., Luo, Y., & Field, C. B. (2003). Nitrogen and climate
784 change. *Science*, *302*(5650), 1512–1513. https://doi.org/10.1126/science.1091390
785 Inderjit, Wardle, D. A., Karban, R., & Callaway, R. M. (2011). The ecosystem and evolutionary
786 contexts of allelopathy. *Trends in Ecology and Evolution*, *26*(12), 655–662.
787 https://doi.org/10.1016/j.tree.2011.08.003
788 Kalisz, S., Kivlin, S. N., & Bialic-Murphy, L. (2021). Allelopathy is pervasive in invasive plants.
789 *Biological Invasions*, *23*(2), 367–371. https://doi.org/10.1007/s10530-020-02383-6
790 Kattge, J., & Knorr, W. (2007). Temperature acclimation in a biochemical model of
791 photosynthesis: a reanalysis of data from 36 species. *Plant, Cell & Environment*, *30*(9),
792 1176–1190. https://doi.org/10.1111/j.1365-3040.2007.01690.x
793 Kenward, M. G., & Roger, J. H. (1997). Small sample inference for fixed effects from restricted
794 maximum likelihood. *Biometrics*, *53*(3), 983. https://doi.org/10.2307/2533558
795 Kummel, M., & Salant, S. W. (2006). The economics of mutualisms: Optimal utilization of
796 mycorrhizal mutualistic partners by plants. *Ecology*, *87*(4), 892–902.
797 https://doi.org/10.1890/0012-9658(2006)87[892:TEOMOU]2.0.CO;2
798 Lajtha, K., Driscoll, C. T., Jarrell, W. M., & Elliott, E. T. (1999). Soil phosphorus. In *Standard*
799 *Soil Methods for Long-Term Ecological Research* (p. 115).
800 Lenth, R. (2019). *emmeans: estimated marginal means, aka least-squares means*. https://cran.r-
801 project.org/package=emmeans
802 Lu, J., Yang, J., Keitel, C., Yin, L., Wang, P., Cheng, W., & Dijkstra, F. A. (2022). Belowground
803 carbon efficiency for nitrogen and phosphorus acquisition varies between *Lolium perenne*
804 and *Trifolium repens* and depends on phosphorus fertilization. *Frontiers in Plant Science*,
805 *13*, 1–9. https://doi.org/10.3389/fpls.2022.927435
806 Medlyn, B. E., Dreyer, E., Ellsworth, D. S., Forstreuter, M., Harley, P. C., Kirschbaum, M. U. F.,
807 Le Roux, X., Montpied, P., Strassemeyer, J., Walcroft, A., Wang, K., & Loustau, D. (2002).
808 Temperature response of parameters of a biochemically based model of photosynthesis. II.
809 A review of experimental data. *Plant, Cell & Environment*, *25*(9), 1167–1179.
810 https://doi.org/10.1046/j.1365-3040.2002.00891.x
811 Menne, M. J., Durre, I., Vose, R. S., Gleason, B. E., & Houston, T. G. (2012). An overview of
812 the global historical climatology network-daily database. *Journal of Atmospheric and*
813 *Oceanic Technology*, *29*(7), 897–910. https://doi.org/10.1175/JTECH-D-11-00103.1

814 Mutz, J., Heberling, J. M., Kivlin, S. N., Smith, N. G., Chatterjee, S., Perkowski, E. A., Bialic-
815 Murphy, L., & Kalisz, S. (n.d.). *Allelopathic invader alters belowground plant-fungal*
816 *interactions, physiology, and biomass allocation in native understory species*.
817 Niinemets, Ü., Kull, O., & Tenhunen, J. D. (1998). An analysis of light effects on foliar
818 morphology, physiology, and light interception in temperate deciduous woody species of
819 contrasting shade tolerance. *Tree Physiology*, *18*(10), 681–696.
820 Niinemets, Ü., & Tenhunen, J. D. (1997). A model separating leaf structural and physiological
821 effects on carbon gain along light gradients for the shade-tolerant species *Acer saccharum*.
822 *Plant, Cell and Environment*, *20*(7), 845–866. https://doi.org/10.1046/j.1365-
823 3040.1997.d01-133.x
824 Onoda, Y., Wright, I. J., Evans, J. R., Hikosaka, K., Kitajima, K., Niinemets, Ü., Poorter, H.,
825 Tosens, T., & Westoby, M. (2017). Physiological and structural tradeoffs underlying the
826 leaf economics spectrum. *New Phytologist*, *214*(4), 1447–1463.
827 https://doi.org/10.1111/nph.14496
828 Paillassa, J., Wright, I. J., Prentice, I. C., Pepin, S., Smith, N. G., Ethier, G., Westerband, A. C.,
829 Lamarque, L. J., Wang, H., Cornwell, W. K., & Maire, V. (2020). When and where soil is
830 important to modify the carbon and water economy of leaves. *New Phytologist*, *228*(1),
831 121–135. https://doi.org/10.1111/nph.16702
832 Palecki, M., Durre, I., Applequist, S., Arguez, A., & Lawrimore, J. H. (2021). U.S. Climate
833 Normals 2020: U.S. Hourly Climate Normals (1991-2020). *NOAA National Centers for*
834 *Environmental Information*.
835 Perkowski, E. A., Terrones, J., German, H. L., & Smith, N. G. (2024). Symbiotic nitrogen
836 fixation reduces belowground biomass carbon costs of nitrogen acquisition under low, but
837 not high, nitrogen availability. *AoB PLANTS*, *16*(5), 1–22.
838 https://doi.org/10.1093/aobpla/plae051
839 Perkowski, E. A., Waring, E. F., & Smith, N. G. (2021). Root mass carbon costs to acquire
840 nitrogen are determined by nitrogen and light availability in two species with different
841 nitrogen acquisition strategies. *Journal of Experimental Botany*, *72*(15), 5766–5776.
842 https://doi.org/10.1093/jxb/erab253

Qu, T., Du, X., Peng, Y., Guo, W., Zhao, C., & Losapio, G. (2021). Invasive species allelopathy decreases plant growth and soil microbial activity. *PLoS ONE*, *16*(2 February), 1–12. https://doi.org/10.1371/journal.pone.0246685

R Core Team. (2021). *R: A language and environment for statistical computing* (4.1.1). R Foundation for Statistical Computing. https://www.r-project.org/

Rastetter, E. B., Vitousek, P. M., Field, C. B., Shaver, G. R., Herbert, D., & Ågren, G. I. (2001). Resource optimization and symbiotic nitrogen fixation. *Ecosystems*, *4*(4), 369–388. https://doi.org/10.1007/s10021-001-0018-z

Reich, P. B. (2014). The world-wide 'fast-slow' plant economics spectrum: a traits manifesto. *Journal of Ecology*, *102*(2), 275–301. https://doi.org/10.1111/1365-2745.12211

Roche, M. D., Pearse, I. S., Bialic-Murphy, L., Kivlin, S. N., Sofaer, H. R., & Kalisz, S. (2021). Negative effects of an allelopathic invader on AM fungal plant species drive community-level responses. *Ecology*, *102*(1), 1–12. https://doi.org/10.1002/ecy.3201

Roche, M. D., Pearse, I. S., Sofaer, H. R., Kivlin, S. N., Spyreas, G., Zaya, D. N., & Kalisz, S. (2023). Invasion-mediated mutualism disruption is evident across heterogeneous environmental conditions and varying invasion intensities. *Ecography*, *2023*(7), 1–11. https://doi.org/10.1111/ecog.06434

Rodgers, V. L., Stinson, K. A., & Finzi, A. C. (2008). Ready or not, garlic mustard is moving in: *Alliaria petiolata* as a member of eastern north American forests. *BioScience*, *58*(5), 426–436. https://doi.org/10.1641/B580510

Saathoff, A. J., & Welles, J. (2021). Gas exchange measurements in the unsteady state. *Plant Cell and Environment*, *44*(11), 3509–3523. https://doi.org/10.1111/pce.14178

Smith, N. G., & Dukes, J. S. (2018). Drivers of leaf carbon exchange capacity across biomes at the continental scale. *Ecology*, *99*(7), 1610–1620. https://doi.org/10.1002/ecy.2370

Smith, N. G., Keenan, T. F., Prentice, I. C., Wang, H., Wright, I. J., Niinemets, Ü., Crous, K. Y., Domingues, T. F., Guerrieri, R., Ishida, F. Y., Kattge, J., Kruger, E. L., Maire, V., Rogers, A., Serbin, S. P., Tarvainen, L., Togashi, H. F., Townsend, P. A., Wang, M., … Zhou, S.-X. (2019). Global photosynthetic capacity is optimized to the environment. *Ecology Letters*, *22*(3), 506–517. https://doi.org/10.1111/ele.13210

Smith, S. E., & Read, D. J. (2008). *Mycorrhizal Symbiosis*.

873 Tejera-Nieves, M., Seong, D. Y., Reist, L., & Walker, B. J. (2024). The Dynamic Assimilation
874 Technique measures photosynthetic CO_2 response curves with similar fidelity to steady-
875 state approaches in half the time. *Journal of Experimental Botany*, *75*(10), 2819–2828.
876 https://doi.org/10.1093/jxb/erae057
877 Treseder, K. K. (2004). A meta-analysis of mycorrhizal responses to nitrogen, phosphorus, and
878 atmospheric CO_2 in field studies. *New Phytologist*, *164*(2), 347–355.
879 https://doi.org/10.1111/j.1469-8137.2004.01159.x
880 USDA NRCS. (2022). The PLANTS Database. *(Http://Plants.Usda.Gov, 18 November 2022).*
881 *National Plant Data Team, Greensboro, NC 27401-4901 USA.*
882 van Diepen, L. T. A., Lilleskov, E. A., Pregitzer, K. S., & Miller, R. M. (2007). Decline of
883 arbuscular mycorrhizal fungi in northern hardwood forests exposed to chronic nitrogen
884 additions. *New Phytologist*, *176*(1), 175–183. https://doi.org/10.1111/j.1469-
885 8137.2007.02150.x
886 Walters, R. G. (2005). Towards an understanding of photosynthetic acclimation. *Journal of*
887 *Experimental Botany*, *56*(411), 435–447. https://doi.org/10.1093/jxb/eri060
888 Waring, E. F., Perkowski, E. A., & Smith, N. G. (2023). Soil nitrogen fertilization reduces
889 relative leaf nitrogen allocation to photosynthesis. *Journal of Experimental Botany*, *74*(17),
890 5166–5180. https://doi.org/10.1093/jxb/erad195
891 Weatherburn, M. W. (1967). Phenol-hypochlorite reaction for determination of ammonia.
892 *Analytical Chemistry*, *39*(8), 971–974. https://doi.org/10.1021/ac60252a045
893 Westerband, A. C., Wright, I. J., Maire, V., Paillassa, J., Prentice, I. C., Atkin, O. K.,
894 Bloomfield, K. J., Cernusak, L. A., Dong, N., Gleason, S. M., Guilherme Pereira, C.,
895 Lambers, H., Leishman, M. R., Malhi, Y., & Nolan, R. H. (2023). Coordination of
896 photosynthetic traits across soil and climate gradients. *Global Change Biology*, *29*(3), 856–
897 873. https://doi.org/10.1111/gcb.16501
898 Wild, J., Kopecký, M., Macek, M., Šanda, M., Jankovec, J., & Haase, T. (2019). Climate at
899 ecologically relevant scales: A new temperature and soil moisture logger for long-term
900 microclimate measurement. *Agricultural and Forest Meteorology*, *268*(July 2018), 40–47.
901 https://doi.org/10.1016/j.agrformet.2018.12.018
902 Wright, I. J., Reich, P. B., Westoby, M., Ackerly, D. D., Baruch, Z., Bongers, F., Cavender-
903 Bares, J., Chapin, T., Cornelissen, J. H. C., Diemer, M., Flexas, J., Garnier, E., Groom, P.

K., Gulias, J., Hikosaka, K., Lamont, B. B., Lee, T. D., Lee, W., Lusk, C. H., … Villar, R. (2004). The worldwide leaf economics spectrum. *Nature*, *428*(6985), 821–827. https://doi.org/10.1038/nature02403

Zhang, Z., Liu, Y., Yuan, L., Weber, E., & van Kleunen, M. (2021). Effect of allelopathy on plant performance: a meta-analysis. *Ecology Letters*, *24*(2), 348–362. https://doi.org/10.1111/ele.13627

Supporting Information

Table S1 Analysis of variance results exploring the role of *A. petiolata* treatment and measurement period on soil nutrient availabilities

Table S2 Analysis of variance results exploring the role of *A. petiolata* treatment and day of year on soil moisture

Figure S1 Effects of *A. petiolata* treatment and tree canopy status on soil nitrate and ammonium availability

Figure S2 Effects of *A. petiolata* treatment and tree canopy status on relative chlorophyll content in *Trillium* spp. and *M. racemosum*.

SUPPLEMENTAL MATERIAL for "Negative effects of allelopathic plant invasion accumulate as the growth season progresses"

Table S1 Analysis of variance results exploring the role of *A. petiolata* treatment and measurement period on soil nitrogen and phosphorus availability*

		Soil nitrogen availability		**Soil NO_3-N availability**		**Soil NH_4-N availability**	
	df	χ^2	*p*	χ^2	*p*	χ^2	*p*
A. petiolata treatment (A)	1	0.538	0.463	2.334	0.127	1.430	0.232
Canopy status (C)	1	53.915	**<0.001**	67.788	**<0.001**	0.010	0.920
A*C	1	1.279	0.258	2.028	0.154	5.383	**0.020**

		Soil phosphate availability		**Soil N:P**	
	df	χ^2	*p*	χ^2	*p*
A. petiolata treatment (A)	1	2.859	*0.091*	3.790	*0.052*
Canopy status (C)	1	11.028	**0.001**	25.264	**<0.001**
A*C	1	0.358	0.549	0.722	0.396

*Significance determined using Type II Wald χ^2 tests (α=0.05). *P*-values less than 0.05 are in bold, while $0.05<p<0.1$ are in italic font. Key: df = degrees of freedom

Table S2 Analysis of variance results exploring the role of *Alliaria* treatment on volumetric soil moisture content across the measurement period*

	χ^2	*p*
Alliaria treatment (A)	17.778	**<0.001**
Day of year (D)	310.951	**<0.001**
A*D	0.272	0.602

*Significance determined using Type II Wald χ^2 tests (α=0.05). *P*-values less than 0.05 are in bold.

Figure S1

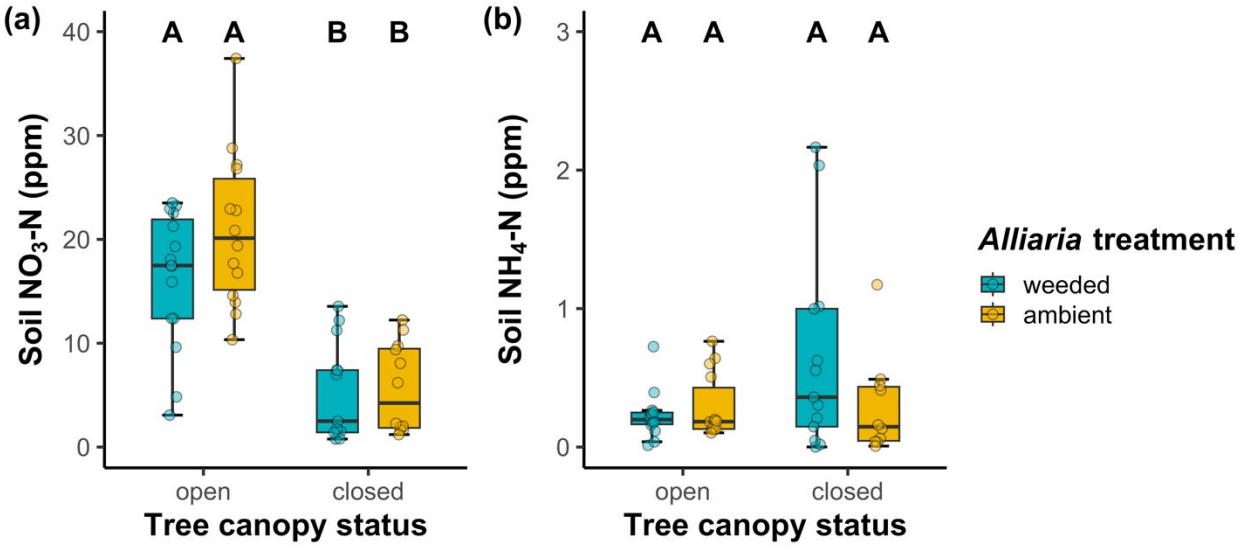

Figure S1 Effects of *A. petiolata* treatment and tree canopy status on soil nitrate availability (a) and soil ammonium availability (b). Tree canopy status is on the x-axis. Teal points and boxplots indicate measurements collected in plots where *A. petiolata* was weeded and gold points and boxplots indicate measurements collected in subplots where *A. petiolata* was present at ambient levels. Boxes represent the upper (75% percentile) and lower (25% percentile) quartiles, and whiskers represent 1.5 times the upper and lower quartile values. Lettering above each treatment group indicates statistically different groups where Tukey: $p<0.05$.

Figure S2

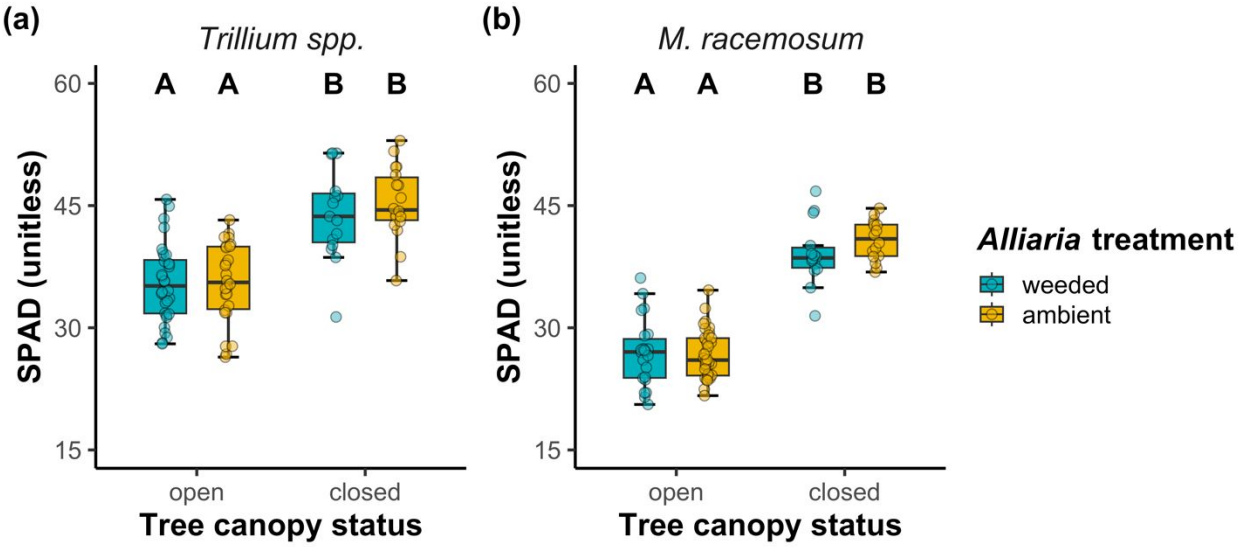

Figure S2 Effects of *A. petiolata* treatment and tree canopy status on relative chlorophyll content in *Trillium* spp. (a) and *M. racemosum* (b). Tree canopy status is on the x-axis. Teal points and boxplots indicate measurements collected in plots where *A. petiolata* was weeded and gold points and boxplots indicate measurements collected in subplots where *A. petiolata* was present at ambient levels. Boxes represent the upper (75% percentile) and lower (25% percentile) quartiles, and whiskers represent 1.5 times the upper and lower quartile values. Lettering above each treatment group indicates statistically different groups where Tukey: $p<0.05$.